Journal of Solid State Chemistry **146,** 506–515 (1999)
Article ID jssc.1999.8413, available online at http://www.idealibrary.com on IDEAL®

Fourier Transform Infrared and Raman Spectroscopic Study of the Local Structure of Mg-, Ni-, and Co-Hydrotalcites

J. Theo Kloprogge[1] and Ray L. Frost

Centre for Instrumental and Developmental Chemistry, Queensland University of Technology, G.P.O. Box 2434, Brisbane Q 4001, Australia

Received February 8, 1999; in revised form May 25, 1999; accepted May 27, 1999

Synthetic Mg-, Ni- (takovite), and Co-hydrotalcite are characterized by FT-IR and FT-Raman spectroscopy. Changes in the composition brought about by changing the divalent metal result in small but significant changes in band positions of the modes related to the hydroxyl groups, as each hydroxyl group in the hydrotalcite structure is coordinated to three metal cations. It has also a similar effect on the interlayer water and carbonate band positions as evidenced by small shifts in band positions and the occurrence of doublets, especially for the interlayer carbonate ions. The carbonate doublets are due to site symmetry lowering. © 1999 Academic Press

***Key Words*: anionic clay; FT-IR spectroscopy; FT-Raman spectroscopy; hydrotalcite; layered double hydroxide; takovite.**

INTRODUCTION

Hydrotalcites found in nature are known as the pyroaurite-sjögrenite group. The structure of hydrotalcite, also known as anionic clays or layered double hydroxides (LDH), can be visualized as positively charged OH-layers comparable to those in brucite ($Mg(OH)_2$) in which a part of the Mg^{2+} is substituted by a trivalent metal like Al^{3+} separated by charge compensating, mostly hydrated, anions between the OH-layers. In hydrotalcites a range of compositions are possible of the type $[M^{2+}_{1-x}M^{3+}_x(OH)_2][A^{n-}]_{x/n}\cdot yH_2O$, where M^{2+} and M^{3+} are the di- and trivalent cations in the octahedral sites within the OH-layers with x normally between 0.17 and 0.33. A^{n-} is an exchangeable anion. The first hydrotalcites were synthesized by Feitknecht during World War II (1, 2). The structure was first described by Allmann and Taylor (3–6).

Coprecipitation is probably the best technique for the synthesis of hydrotalcites, as it allows homogeneous precursors as starting materials. For coprecipitation it is necessary to work under conditions of supersaturation mostly achieved by variation in pH (7). Two frequently used techniques are coprecipitation at low (8–10) and at high supersaturation (11–13). In this study we used the latter route for the preparation of hydrotalcites with Mg^{2+}, Ni^{2+}, or Co^{2+} combined with Al^{3+} in a molar ratio M^{2+}/M^{3+} of 6/2 and CO_3^{2-} as charge balancing anion.

Infrared and, rarely, Raman spectroscopy have been used for the study of hydrotalcites with different cations and of the anionic pillaring and thermal decomposition of hydrotalcites, but mainly for the study of exchangeable anions, like CO_3^{2-}, Cl^-, ClO_4^-, NO_3^-, SO_4^{2-}, and CrO_4^{2-} (8, 9, 13, 14) and but also larger groups as anionic silica $SiO(OH)_3^-$ (15) and larger polyoxometalate ions or $Fe(CN)_6^{n-}$ (16–18). Each of these anions shows specific infrared or Raman bands; e.g., carbonate is characterized by a double peak around 1360 and 1400 cm^{-1} and peaks at 880 and 680 cm^{-1} (19).

Many variations in divalent/trivalent metal compositions have been reported for hydrotalcites (7). Nowadays a vast amount of literature describes the synthesis of takovite, a hydrotalcite in which Mg^{2+} is replaced by Ni^{2+}, e.g., (11, 14, 20–29). Takovite is an important precursor for the preparation of Ni/Al_2O_3 catalysts (30–38). A much smaller number of papers describe the use of Mg-hydrotalcite as a catalyst precursor. Suzuki and co-workers described an aldol condensation reaction over a heat-treated Mg-hydrotalcite containing various interlayer anions and for halide-exchange reactions between alkyl halides (39, 40). Corma *et al.* (41) reported the condensation of benzaldehyde with ethyl acetoacetate over a calcined Mg-hydrotalcite together with a range of side-reactions caused by the basicity of the calcined hydrotalcite. Cobalt plays an important role in heterogeneous catalysis, and therefore the incorporation of cobalt in hydrotalcites has been described for the preparation of mixed metal oxide catalysts. In the simplest case the Mg^{2+} in the hydrotalcite is replaced by Co^{2+} (42–45). This type of catalyst has mainly been tested for Fischer–Tropsch reactions (44, 45). Or the cobalt was added as an extra metal to hydrotalcites in which Mg and Al were replaced by other divalent and/or trivalent metals (46–48).

The infrared spectra from hydrotalcites with Mg partly or completely replaced by Ni, Co, and Zn have been briefly

[1] To whom correspondence should be addressed. Fax: +61 7 3864 1804. E-mail: t.kloprogge@qut.edu.au.

0022-4596/99 $30.00

reported. Recently, we have described assignments of the infrared and Raman spectra at room temperature and *in situ* during heat-treatment by infrared emission spectroscopy of $(Mg,Zn)_6Al_2(OH)_{16}CO_3 \cdot nH_2O$ (49–52). However, detailed descriptions of the influence of different cations on the Raman and IR spectra, especially on the lattice region, of Ni- and Co-hydrotalcite have not been published. Therefore, this paper, following our work on hydrotalcites (51, 52), aims at a detailed description of hydrotalcites containing Mg, Ni, or Co.

EXPERIMENTAL

The hydrotalcites with theoretical compositions of $Mg_6Al_2(OH)_{16}CO_3 \cdot nH_2O$, $Ni_6Al_2(OH)_{16}CO_3 \cdot nH_2O$, and $Co_6Al_2(OH)_{16}CO_3 \cdot nH_2O$ were synthesized according to the method described before by Kloprogge and co-workers for the synthesis of three-metal hydrotalcites $(Mg,Zn)_6Al_2(OH)_{16}CO_3 \cdot nH_2O$ (49–52). This method comprises the slow simultaneous addition of a mixed aluminum nitrate (0.25 M)–magnesium nitrate (0.75 M), aluminum nitrate (0.25 M)–nickel chloride (0.75 M), or aluminum nitrate (0.25 M)–cobalt chloride (0.75 M) solution and a mixed NaOH (2.00 M)–Na_2CO_3 (0.125 M) solution under vigorous stirring, buffering the pH at a value above 10. The products were washed to eliminate excess salt and dried at 60°C.

The nature of the resulting material was checked by X-ray powder diffraction (XRD). The XRD analyses were carried out on a Philips wide-angle PW 1050/25 vertical goniometer equipped with a graphite diffracted beam monochromator. The *d*-values and intensity measurements were improved by application of an in-house-developed computer-aided divergence slit system enabling constant sampling area irradiation (20 mm long) at any angle of incidence. The goniometer radius was enlarged to 204 mm. The radiation applied was Co$K\alpha$ from a long fine-focus Co tube operating at 35 kV and 40 mA. The samples were measured at 50% relative humidity in stepscan mode with steps of 0.02° 2θ and a counting time of 2 s.

The Fourier transform Raman spectroscopy (FT-Raman) analyses were performed on a Perkin–Elmer System 2000 Fourier transform spectrometer equipped with a Raman accessory comprising a Spectron Laser Systems SL301 Nd:YAG laser operating a wavelength of 1064 nm. Spectral manipulation such as baseline adjustment, smoothing, and normalization were performed using the Spectracalc software package GRAMS (Galactic Industries Corporation, NH, USA). Band component analysis was undertaken using the Jandel "Peakfit" software package, which enabled the type of fitting function to be selected and allows specific parameters to be fixed or varied accordingly. Band fitting was done using a Lorentz–Gauss cross-product function with the minimum number of component bands used for the fitting process. The Gauss–Lorentz ratio was maintained at values greater than 0.7, and fitting was undertaken until reproducible results were obtained with squared correlations of r^2 greater than 0.995.

The hydrotalcites were oven dried to remove any adsorbed water and stored in a desiccator before measurement in the FT-IR spectrometer. The sample (1 mg) was finely ground for one minute, combined with oven dried spectroscopic grade KBr having a refractive index of 1.559 and a particle size of 5–20 μm (250 mg), and pressed into a disc under vacuum. The spectrum of each sample was recorded in triplicate by accumulating 64 scans at 4 cm^{-1} resolution between 400 and 4000 cm^{-1} using the Perkin–Elmer 1600 series Fourier transform infrared spectrometer equipped with a LITA detector. Data interpretation and manipulation was carried out using the Spectracalc software package GRAMS (Galactic Industries Corporation, NH, USA) and Microsoft Excel. Band component analysis was undertaken using the Jandel "Peakfit" software package which enabled the type of fitting function to be selected and allows specific parameters to be fixed or varied accordingly. Band fitting was done using a Lorentz–Gauss cross-product function with the minimum number of component bands used for the fitting process. The Gauss–Lorentz ratio was maintained at values greater than 0.7, and fitting was undertaken until reproducible results were obtained with squared correlations of r^2 greater than 0.995.

RESULTS AND DISCUSSION

X-Ray Diffraction

Figure 1 shows the XRD patterns of the Mg-, Ni-(takovite), and Co-hydrotalcites. The (00*l*) reflections (003), (006), and (009) are easily recognized, although the last one shows overlap with the (012) and (015) reflections resulting in a broad signal between 40 and 45° 2θ. Furthermore, the two reflections of (110) and (113) can be clearly distinguished between 70° and 75° 2θ. The (00l) reflections are characterized by high intensities combined with broad lineshapes indicating that the hydrotalcites are of relatively high crystallinity but with very small crystallites. No other crystalline phases can be detected in the XRD patterns, indicating that all three syntheses were successful. Further analysis of the observed XRD patterns revealed small differences in the cell parameters as a function of the composition. Mg-hydrotalcite had an *a*-axis of 3.055 $\pm$ 0.001 Å and a *c*-axis of 23.17 $\pm$ 0.04 Å. Co-hydrotalcite had a slightly bigger *a*-axis of 3.065 $\pm$ 0.006 Å but the same *c*-axis. The takovite, in contrast, showed a smaller *a*-axis of 3.024 $\pm$ 0.005 Å and a larger *c*-axis of 23.48 $\pm$ 0.05 Å. The substitution of Mg with an ionic radius of 0.65 Å by the larger Co with an ionic radius of 0.74 Å is thought to be causing the increase in the *a*-axis. Ni, however, has an ionic radius of 0.72 Å, very close to that of Co, but the *a*-axis of the takovite is much smaller

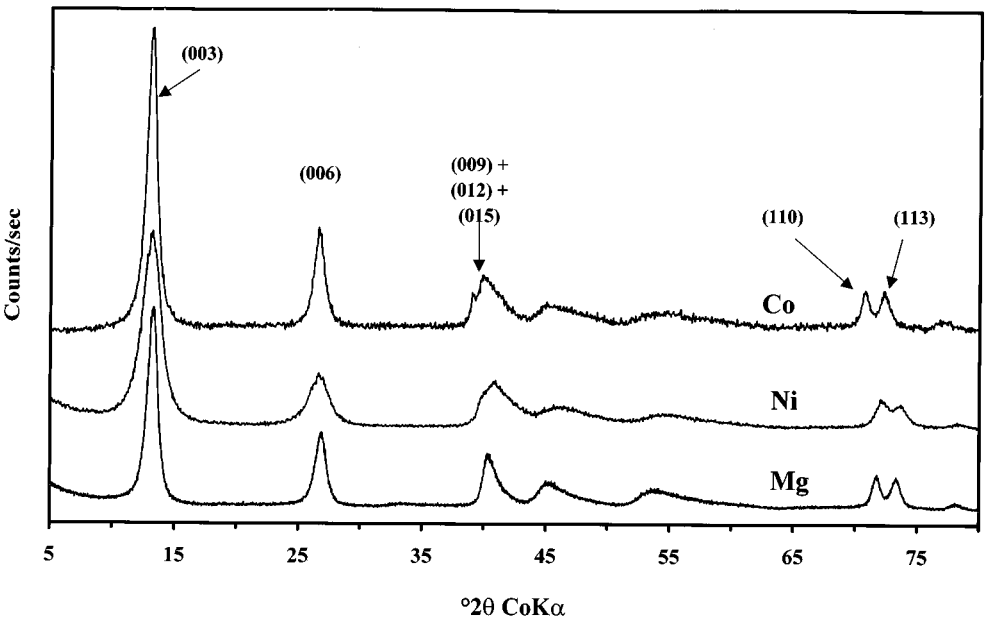

FIG. 1. X-ray diffraction patterns of the divalent metal hydrotalcites, Mg, Ni, and Co.

although in agreement with the literature value of 3.025 Å, while the *c*-axis is significantly bigger. The *c*-axis is also bigger than the value of 22.59 Å reported for takovite in the literature (7).

FT-IR Spectroscopy

Figure 2 displays the infrared spectra of the Mg-, Ni-, and Co-hydrotalcites in the region between 400 and 4000 cm^{-1}. Band component analysis of the hydroxyl-stretching region between 2500 and 3900 cm^{-1} reveals the presence of four bands (Fig. 3). In general the band observed around 2950–3050 cm^{-1} is interpreted as the CO_3^{2-}–H_2O bridging mode of carbonate and water in the interlayer (8, 29, 51). There seems to be a very small influence by the hydroxide layer composition as indicated by a shift in the band position from 2972 cm^{-1} for the Mg-hydrotalcite to 2973 cm^{-1} for the Ni-hydrotalcite and to 2981 cm^{-1} for the Co-hydrotalcite.

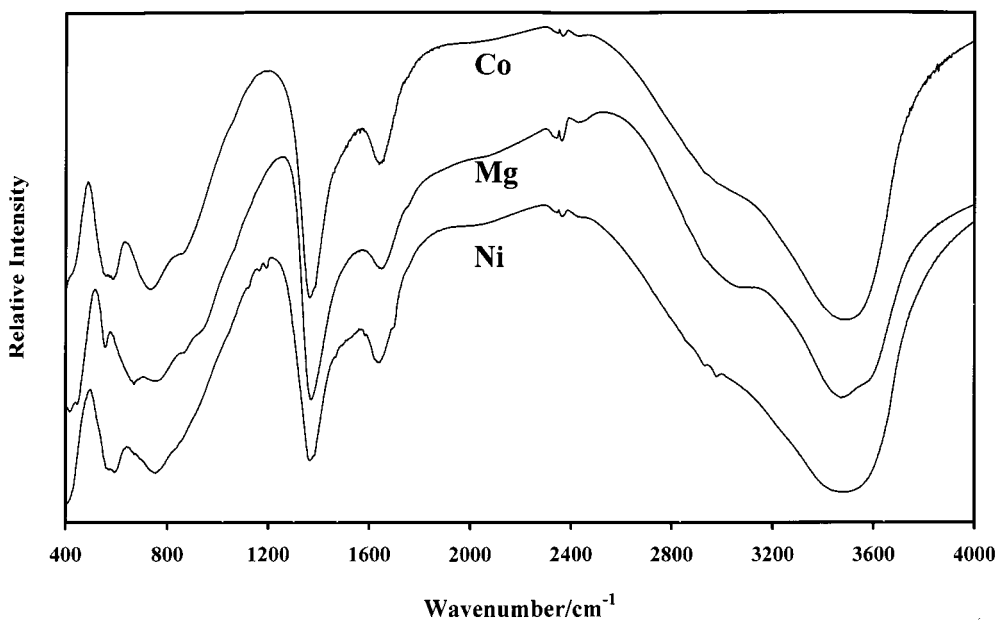

FIG. 2. FT-IR spectra of hydrotalcites with Mg, Co, and Ni in the region 400–4000 cm^{-1}.

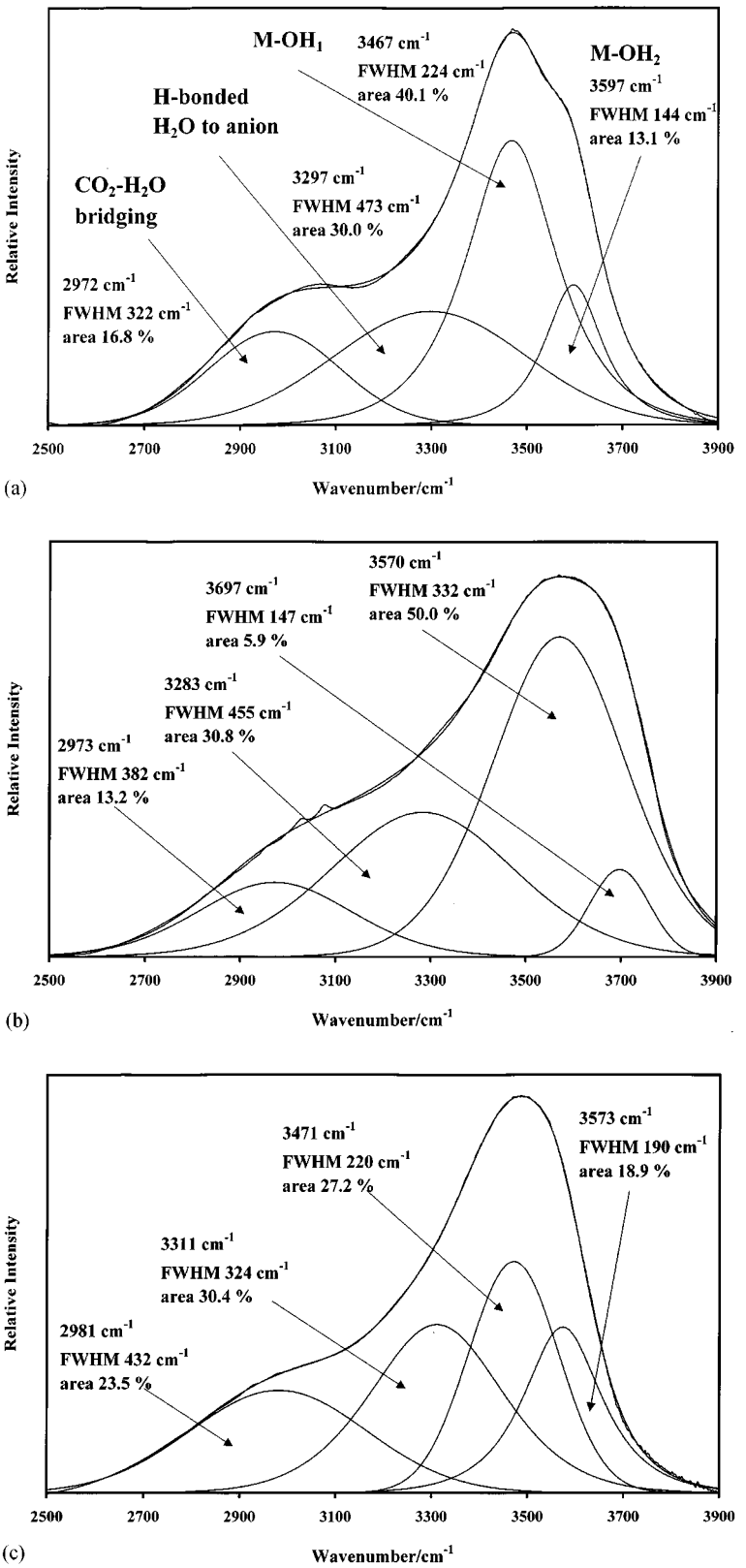

FIG. 3. (a) Band component analysis of the FT-IR spectrum of Mg-hydrotalcite in the region 2500–3900 cm^{-1}. (b) Band component analysis of the FT-IR spectrum of Ni-hydrotalcite in the region 2500–3900 cm^{-1}. (c) Band component analysis of the FT-IR spectrum of Co-hydrotalcite in the region 2500–3900 cm^{-1}.

TABLE 1
Band Assignment of the Hydroxyl Stretching Modes

Mg-hydrotalcite	Ni-hydrotalcite	Co-hydrotalcite	Brucite[a] $Mg(OH)_2$	Gibbsite[a] $Al(OH)_3$	Heterogenite[a] CoO(OH)	Assignment for hydrotalcites
		3471		3380–3436	3400	"Co"–OH
3467				3445–3428		"Al"–OH
3597	3570	3573	3570	3520–3527		"Mg"–OH/"Al"–OH
				3617–3623		
	3697			3661–3685		"Al"–OH/"Ni"–OH

[a] Based on (53–55).

The second band assigned to hydrogen-bonded interlayer water around 3300 cm^{-1} (8, 29, 51) shows a similar trend. The remaining two bands represent different M–OH stretching modes. Based on the crystal structure of hydrotalcite, it can be argued that each OH group is coordinated to three metal cations. In the case of hydrotalcite with a M^{2+}/M^{3+} ratio of 3 this means that one stretching mode probably truly reflects a M^{2+}–OH bonding while the other one is more an intermediate between an M^{2+}–OH and an M^{3+}–OH. Comparison with pure $M^{2+}(OH)_2$ and $M^{3+}(OH)_3$ will show a shift in the band positions. Infrared spectra of the various hydrotalcites reported in the literature only display a very broad band around 3400–3500 cm^{-1}, without any evidence for multiple bands based on the presence of shoulders and asymmetry of the band (20, 22, 28, 42). Furthermore, none of these papers reports band component analysis results as in this paper. Based on the band component analysis of the spectra of the hydrotalcites and the comparison with simple hydroxides, a more detailed assignment is possible (Table 1). The band at 3467 cm^{-1} for the Mg-hydrotalcite seems to be mainly due to the Al–OH bond with only a small influence of nearby Mg cations causing a small shift to higher frequency. The other band can not be clearly assigned to either Mg- or Al–OH and probably represents a hydroxyl coordinated by both metals. A similar reasoning is true for the Ni- and Co-hydrotalcite. The lowest frequency band represents mainly the influence of the bivalent metal on the hydroxyl group whereas the higher frequency band is of a more mixed nature, where both the divalent and trivalent metal influences the hydroxyl group. Comparison of the Ni- and Co-hydrotalcite spectra with the Mg-hydrotalcite spectrum shows a trend from around 3570–3575 cm^{-1} to around 3600 cm^{-1}, which can be explained mainly by the difference in the mass of the cations involved and by the difference in bond-strength between the cations and adjacent oxygen atoms. Generally, the band positions are reciprocally related to the bond-strength of the cation to oxygen atoms, which fits well with the observed differences between the Mg- and the Ni- and Co-hydrotalcites as the bond-strength increases approximately 12.5% from Mg–O to Ni/Co–O (Mg–O approximately 330 kJ/mol, Ni–O approximately 372 kJ/mol, and Co–O approximately 368 kJ/mol).

Figure 4 displays the low frequency region of all three hydrotalcites. This region of the infrared spectrum has been reported for Co-hydrotalcite by Kannan and Swamy (42), but they did not give a band assignment for this region. The same is true for takovite or Ni-hydrotalcite; various papers show the spectrum but do not even report the band positions (see, e.g., (20–22, 27, 28)). The assignment in this paper mainly follows the assignment given for Mg-hydrotalcite by Kloprogge and co-workers (51). Based on comparison with their work the bands around 553 and 755 cm^{-1} can be assigned to translation modes of the hydroxyl groups mainly influenced by the trivalent aluminum. The corresponding deformation modes are observed as two bands around 925 and 1010–1055 cm^{-1}. The exact positions of these bands for the various hydrotalcites are influenced by the divalent metal present in the structure. The bands observed at 635, 597, and 588 cm^{-1} for the Mg-, Ni-, and Co-hydrotalcite are interpreted as being hydroxyl translation modes mainly influenced by the divalent metal in the hydrotalcite structure. Similar to the shift observed in the hydroxyl stretching region for the hydroxyl bands related to the divalent cations in the hydrotalcite structure due to changes in mainly the bond-strength and atomic weight, the bands shift by approximately 50 cm^{-1} from around 580–600 cm^{-1} for the Ni/Co related OH translation modes to 635 cm^{-1} for the Mg related OH translation modes. The two bands around 660 and 860 cm^{-1} are characteristic for the v_4 and v_2 modes of the interlayer carbonate group (51). The shift in the positions of these two modes depending on the metal content of the hydrotalcite indicates that the divalent metal influences the exact nature of the interlayer carbonate, in accordance with the observations described above for the hydroxyl stretching region. (See Table 2.)

The region roughly between 1200 and 1800 cm^{-1} for Mg-hydrotalcite is characterized by the bending mode of interlayer water around 1655 cm^{-1} and the two v_3 modes (symmetric stretch) at 1365 and 1401 cm^{-1} associated with the interlayer carbonate (51, 52). Figure 5 shows the band component analysis of this region for all three hydrotalcites.

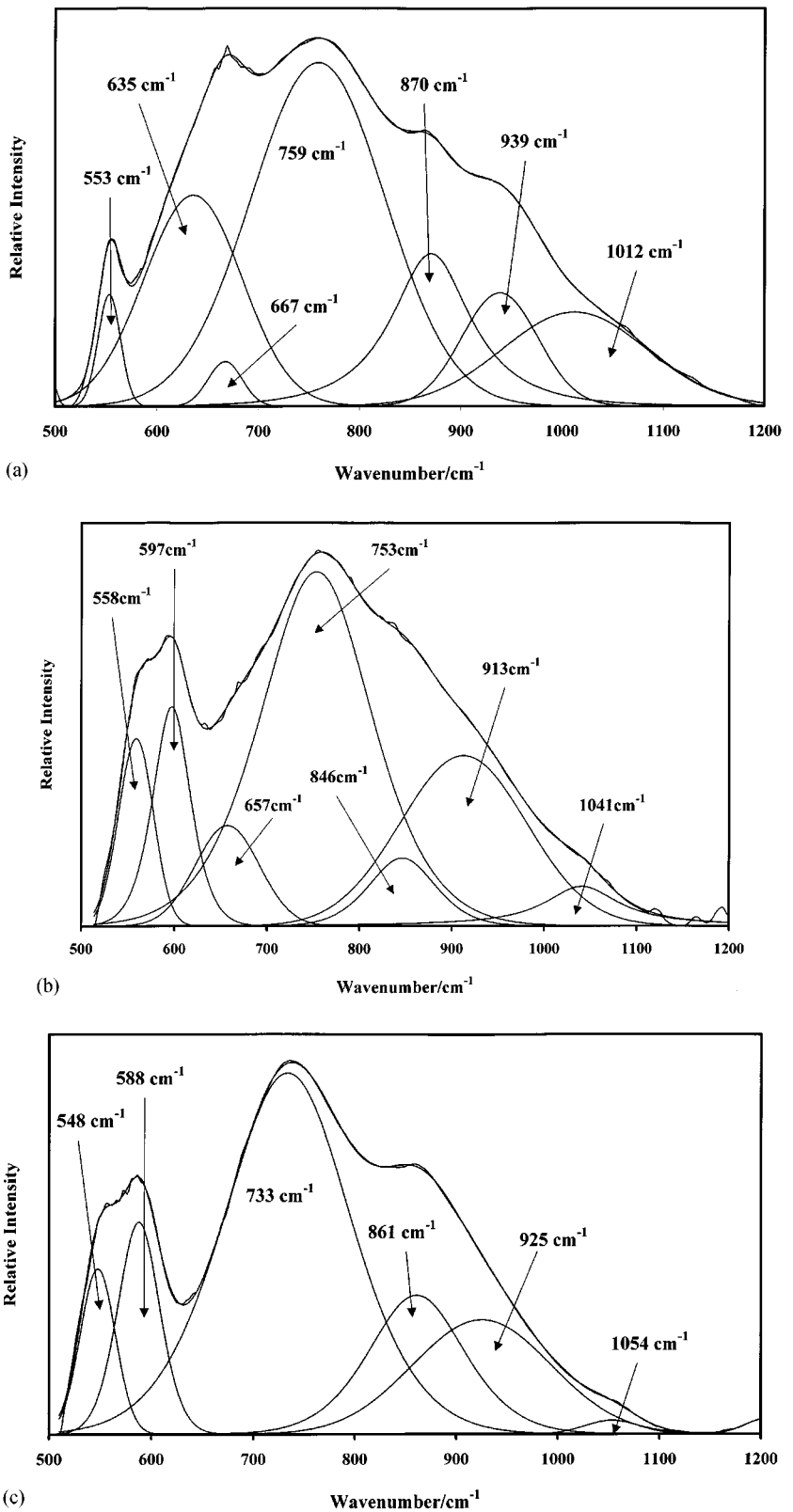

FIG. 4. (a) Band component analysis of the FT-IR spectrum of Mg-hydrotalcite in the region 500–1200 cm^{-1}. (b) Band component analysis of the FT-IR spectrum of Ni-hydrotalcite in the region 500–1200 cm^{-1}. (c) Band component analysis of the FT-IR spectrum of Co-hydrotalcite in the region 500–1200 cm^{-1}.

TABLE 2
Band Component Analysis of the Low Frequency Region between 500 and 1200 cm^{-1} of the Infrared Spectra of Mg-, Ni- and Co-hydrotalcite

Mg-hydrotalcite (cm^{-1})	Ni-hydrotalcite (cm^{-1})	Co-hydrotalcite (cm^{-1})	Co-hydrotalcite (42) (cm^{-1})	Assignment
553	558	548	550	"Al"–OH translation
	597	588	600	"Ni"–, "Co"–OH translation
635				"Mg"–OH translation
667	657			v_4 CO_3^{2-}
759	753	733	785	"Al"–OH translation
870	846	861	870	v_2 CO_3^{2-}
939	913	925		doublet "Al"–OH deformation
1012	1041	1054		

These two carbonate modes are only recognizable after band component analysis, and therefore until now a lot of publications only reported a broad band around 1350–1400 cm^{-1} (42, 53). There are two possible explanations for the existence of the double band. Bish and Brindley (20) suggested that the site symmetry of the carbonate ion in the interlayer is lower for takovite compared to sjögrenite, for which they observed only one band. This, however, is not reflected in the Mg-hydrotalcite in this study, which also showed the double band. An alternative explanation was given by Labajos *et al.* (26), who claimed that the splitting of this carbonate mode is due to the fact that there exists some sort of interaction between the carbonate ion and the water molecules in the interlayer and/or the cations (or hydroxyl groups) from the layers causing a decrease in site symmetry. This second interpretation is supported by the results of this study, because there are small but distinct differences in the band positions for both the interlayer water and the carbonate ions depending on the divalent metal present in the hydrotalcite structure. Very interesting is the fact that the interlayer water band at 1643 cm^{-1} for the takovite shows a shoulder belonging to a second band at 1697 cm^{-1}. This band indicates the presence of a small amount of strongly coordinated water to a cation. This may indicated the presence of a very small amount of either nickel or aluminum not incorporated in the hydrotalcite structure, which could not be observed in any other way.

FT-Raman Spectroscopy

Figure 6a shows the low frequency region of the Raman spectrum of Mg-hydrotalcite. Unfortunately, the Ni- and Co-hydrotalcite Raman spectra could not be measured due extensive fluorescence. The low frequency region of the Mg-hydrotalcite Raman spectrum is shown by two small bands around 303 and 388 cm^{-1}. The two much stronger bands around 476 and 552 cm^{-1} are both assigned to hydroxyl groups associated with mainly Al (50, 51) but also influenced by probably one Mg in its coordination. The band at 476 cm^{-1} is only Raman active while the band at 552 cm^{-1} has an equivalent in the infrared spectrum at 553 cm^{-1}. The interlayer carbonate ions can be observed as bands in the Raman spectrum as a very weak v_4 mode at 694 cm^{-1} and a very strong and sharp v_1 at 1061 cm^{-1}. Band component analysis of the v_1 mode shows that it actually contains a second much broader band at a slightly lower frequency of 1053 cm^{-1}. Like for the doublet v_3 in the infrared spectrum, this again is evidence for a lowering of the site symmetry of the interlayer carbonate ion. Theoretically the v_2 and v_3 are only infrared active and not Raman active. However, the Raman spectrum does show a very broad and low intensity band around 1403 cm^{-1}, which coincides with the infrared active v_3 position. This can be explained by the fact that the symmetry lowering of the carbonate interlayer site causes changes in the polarizability, and the originally Raman inactive band can become Raman active although only with very weak intensity.

The hydroxyl-stretching region in the Raman spectrum (Fig. 6b) is slightly more complex than the similar region in the infrared spectrum (Fig. 3a). In addition to the CO_3^{2-}–H_2O bridging mode around 3097 cm^{-1}, the hydrogen-bonded water around 3245 cm^{-1} and the metal–hydroxyl stretching modes around 3454 and 3580 cm^{-1}, which are all Raman and infrared active, an extra band is observed around 3358 cm^{-1}. Based on the present data the assignment of this band is not straightforward. This band can be interpreted either as a third metal–hydroxyl mode or as a second hydrogen-bonded water mode.

CONCLUSIONS

The synthesis of phase pure hydrotalcites containing various divalent metals like Mg, Ni, or Co is relatively simple and results in the formation of good crystalline material.

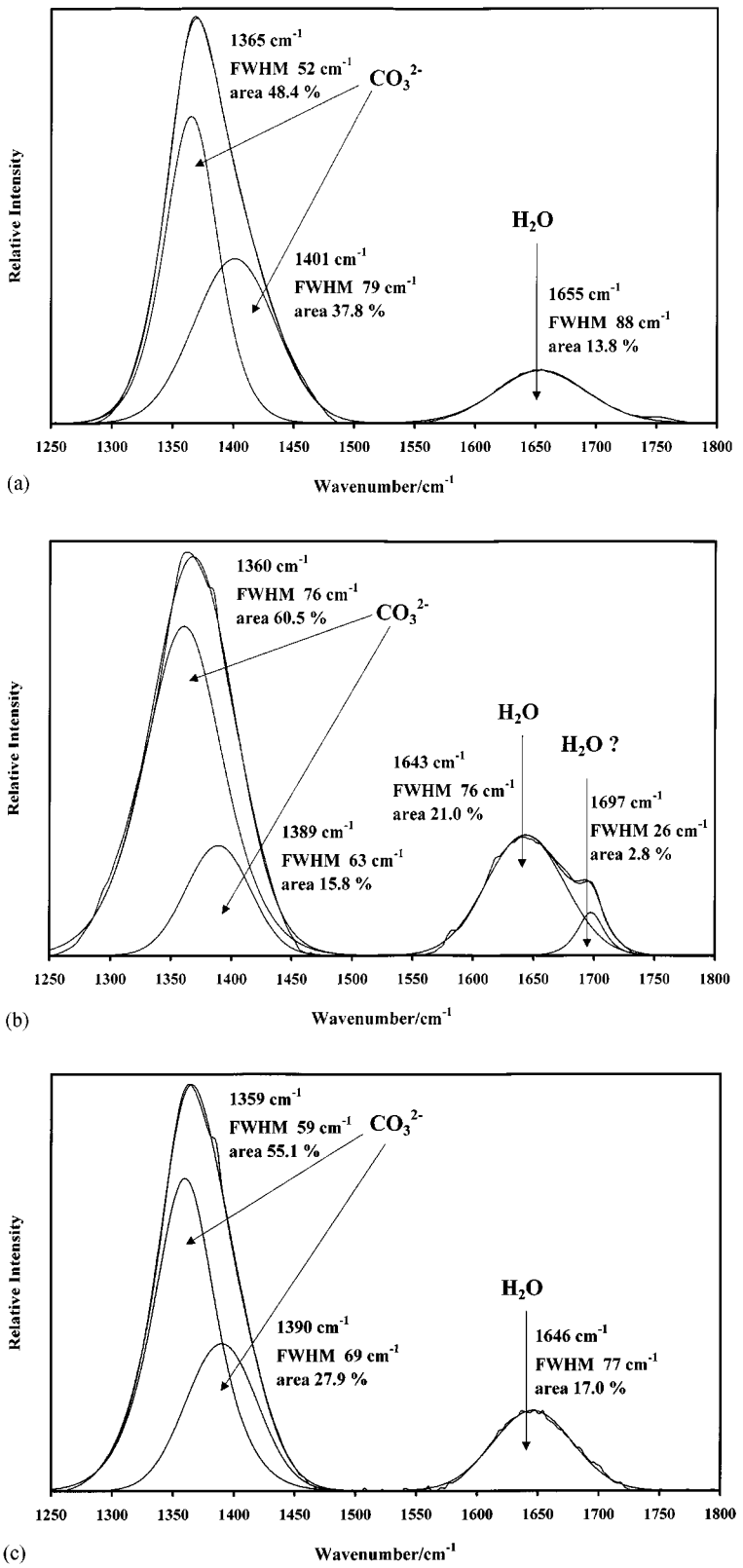

FIG. 5. (a) Band component analysis of the FT-IR spectrum of Mg-hydrotalcite in the region 1250–1800 cm^{-1}. (b) Band component analysis of the FT-IR spectrum of Ni-hydrotalcite in the region 1250–1800 cm^{-1}. (c) Band component analysis of the FT-IR spectrum of Co-hydrotalcite in the region 1250–1800 cm^{-1}.

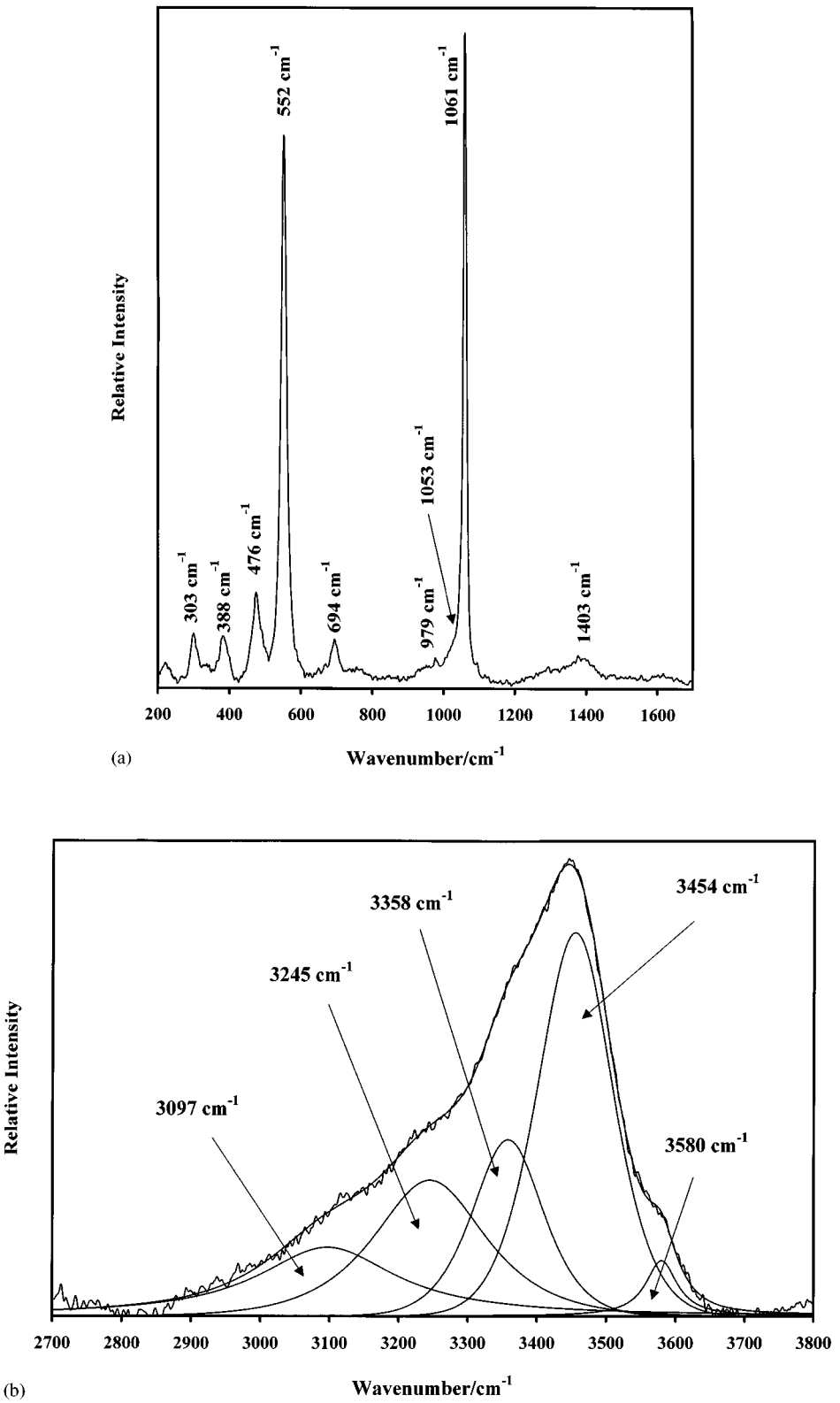

FIG. 6. (a) Raman spectrum of Mg-hydrotalcite in the region 200–1700 cm^{-1}. (b) Raman spectrum and band component analysis of Mg-hydrotalcite in the region 2700–3800 cm^{-1}.

This material is very suitable for detailed spectroscopic investigations resulting in a much more detailed assignment of the bands in both the infrared and the Raman spectra. This study has shown that changes in the composition brought about by changing the divalent metal results in small but significant changes in band positions of the modes related to the hydroxyl groups as expected as each hydroxyl group in the hydrotalcite structure is coordinated to three metal cations. These three cations can all be the same or they can have a mixed nature of both divalent and trivalent cations which will result in a shift in the band position. This study has also shown that changing the divalent cation content in the hydroxide layers has also a small but significant effect on the interlayer water molecules and carbonate anions, as evidenced by small shifts in band positions and the occurrence of doublets, especially for the interlayer carbonate ions.

ACKNOWLEDGMENTS

Natalie Leishman is thanked for her assistance in the synthesis and characterization of some of the hydrotalcites. The financial and infrastructural support of the Queensland University of Technology, Centre for Instrumental and Developmental Chemistry, is gratefully acknowledged.

REFERENCES

1. W. Feitknecht, *Helv. Chim. Acta* **25,** 131 (1942).
2. W. Feitknecht, *Helv. Chim. Acta* **25,** 555 (1942).
3. R. Allmann, *Acta Crystallogr. B* **24,** 972 (1968).
4. H. F. W. Taylor, *Mineral. Mag.* **37,** 338 (1969).
5. R. Allmann, *Chimia* **24,** 99 (1970).
6. H. F. W. Taylor, *Mineral. Mag.* **39,** 377 (1973).
7. F. Cavani, F. Trifirò, and A.Vaccari, *Catal. Today* **11,** 173 (1991).
8. S. Miyata, *Clays Clay Mineral.* **23,** 369 (1975).
9. S. Miyata, *Clays Clay Mineral.* **28,** 50 (1980).
10. S. Miyata and A. Okada, *Clays Clay Mineral.* **25,** 14 (1977).
11. W. T. Reichle, *J. Catal.* **94,** 547 (1985).
12. W. T. Reichle, *Solid State Ionics* **22,** 135 (1986).
13. W. T. Reichle, S. Y. Kang, and D. S. Everhardt, *J. Catal.* **101,** 352 (1986).
14. E. Evana, R. Marchidan, and R. Manaila, *Bull Soc. Chim. Belg.* **101,** 101 (1992).
15. A. Schutz and P. Biloen, *J. Solid State Chem.* **68,** 360 (1987).
16. S. Idemura, E. Suzuki, and Y. Ono, *Clays Clay Mineral.* **37,** 553 (1989).
17. J. Wang, Y. Tian, R.-C. Wang, J. L. Colón, and A. Clearfield, *in* "Synthesis/Characterization and Novel Applications of Molecular Sieve Materials" (R. L. Bedard, T. Bein, M. E. Davis, J. Garces, V. A. Maroni, and G. D. Stucky, Eds.), Mat. Res. Symp. Proc. 233, p. 63, 1991.
18. H. C. B. Hansen and C. B. Koch, *Clays Clay Mineral.* **42,** 170 (1994).
19. M. J. Hernandez-Moreno, M. A. Ulibarri, J. L. Rendon, and C. J. Serna, *Phys. Chem. Minerl.* **12,** 34 (1985).
20. D. L. Bish and G. W. Brindley, *Am. Mineral.* **62,** 458 (1977).
21. G. W. Brindley and S. Kikkawa, *Am. Mineral.* **64,** 836 (1979).
22. D. L. Bish, *Bull. Mineral.* **103,** 170 (1980).
23. D. C. Puxley, I. J. Kitchener, C. Komodromos, and N. D. Parkyns, *in* "Preparation of Catalysts III" (G. Poncelet, P. Grange, and P. A. Jacobs, Eds.), p. 237. Elsevier, Amsterdam, 1983.
24. R. M. Taylor, *Clay Mineral.* **19,** 591 (1984).
25. M. J. Hernandez, M. A. Ulibarri, J. L. Rendón, and C. J. Serna, *Thermochim. Acta* **81,** 311 (1984).
26. F. M. Labajos, V. Rives, and M. A. Ulibarri, *Spectrosc. Lett.* **24,** 499 (1991).
27. O. Clause, M. Gazzano, F. Trifiro, A. Vaccari, and L. Zatorski, *Appl. Catal.* **73,** 217 (1991).
28. K. T. Ehlsissen, A. Delahaye-Vidal, P. Genin, M. Figlarz, and P. Willmann, *J. Mater. Chem.* **3,** 883 (1993).
29. M. K. Titulaer, J. B. H. Jansen, and J. W. Geus, *Clays Clay Mineral.* **42,** 249 (1994).
30. E. B. M. Doesburg, S. Orr, J. R. H. Ross, and L. L. van Reijen, *J. Chem. Soc. Chem. Commun.*, 734 (1977).
31. J. R. H. Ross, M. C. F. Steel, and A. Zeini-Isfahani, *J. Catal.* **52,** 280 (1978).
32. E. C. Kruissink, L. L. van Reijen, and J. R. H. Ross, *J. Chem. Soc. Faraday Trans. 1* **77,** 649 (1981).
33. L. E. Alzamora, J. R. H. Ross, E. C. Kruissink, and L. L. van Reijen, *J. Chem. Soc. Faraday Trans. 1* **77,** 665 (1981).
34. S. D. Jackson, S. J. Thomson, and G. Webb, *J. Catal.* **70,** 249 (1981).
35. E. B. M. Doesburg, H. Hakvoort, H. Schaper, and L. L. van Reijen, *Appl. Catal.* **7,** 85 (1983).
36. E. B. M. Doesburg, P. H. M. de Korte, H. Schaper, and L. L. van Reijen, *Appl. Catal.* **11,** 155 (1984).
37. M. R. Gelsthorpe, K. B. Mok, J. R. H. Ross, and R. M. Sambrook, *J. Molec. Catal.* **25,** 253 (1984).
38. O. Clause, M. Goncalves Coelho, M. Gazzano, D. Mateuzzi, F. Trifiro, and A. Vaccari, *Appl. Clay Sci.* **8,** 169 (1993).
39. E. Suzuki and Y. Ono, *Bull. Chem. Soc. Jpn.* **61,** 1008 (1988).
40. E. Suzuki, M. Okamoto, and Y. Ono, *J. Molec. Catal.* **61,** 283 (1990).
41. A. Corma, V. Fornés, R. M. Martín-Aranda, and F. Rey, *J. Catal.* **134,** 58 (1992).
42. S. Kannan and C. S. Swamy, *J. Mater. Sci. Lett.* **11,** 1585 (1992).
43. M. A. Ulibarri, J. M. Fernández, F. M. Labajos, and V. Rives, *Chem. Mater.* **3,** 626 (1991).
44. L. Bruce, J. Takos, and T. W. Turney, *in* "Symposium on New Catalytic Materials and Techniques," p. 502. Div. Petroleum Chemistry, Amer. Chem. Soc., Washington, DC, 1989.
45. M. Blanchard, H. Derule, and P. Canesson, *Catal. Lett.* **2,** 319 (1989).
46. P. Courty, D. Durand, E. Freund, and A. Sugier, *J. Molec. Catal.* **17,** 241 (1982).
47. G. Fornasari, S. G. F. Trifiro, and A. Vaccari, *Ind. Eng. Chem. Res.* **26,** 1500 (1987).
48. G. Busca, F. Trifiro, and A. Vaccari, *Langmuir* **6,** 1440 (1990).
49. N. Leishman, J. T. Kloprogge, R. Fry, and R. L. Frost, *in* "Proceedings, 16th Biennial Clay Conference of the Australian Clay Minerals Society, June 29–July 1, 1998, Brisbane, Australia" (J. T. Kloprogge, Ed.), p. 58, 1998.
50. N. Leishman, J. T. Kloprogge, and R. L. Frost, *in* "Proceedings, 3rd ACOVS, Sept. 29–Oct. 2 1998, Melbourne, Australia," p. 80, 1998.
51. J. T. Kloprogge, R. L. Frost, and L. Hickey, *Clays Clay Miner.*, in press.
52. J. T. Kloprogge and R. L. Frost, *Phys. Chem. Chem. Phys.* **1,** 1643 (1999).
53. J. A. Gadsden, "Infrared Spectra of Minerals and Related Compounds." Butterworth, London/Brisbane/Scarborough/Wellington Durban, 1975.
54. R. L. Frost, J. T. Kloprogge, S. C. Russell, and J. L. Szetu, *Appl. Spectrosc.* **53,** 423 (1999).
55. R. L. Frost and J. T. Kloprogge, *Spectrochim. Acta*, in press.